

C. GÖRLING[✉]
U. LEINHOS
K. MANN

Comparative studies of absorptance behaviour of alkaline-earth fluorides at 193 nm and 157 nm

Laser-Laboratorium Göttingen, Hans-Adolf-Krebs-Weg 1, 37077 Göttingen, Germany

Received: 21 June 2001/Revised version: 2 November 2001

Published online: 7 February 2002 • © Springer-Verlag 2002

ABSTRACT Absorptance losses in MgF₂, CaF₂ and BaF₂ during 193-nm (DUV) and 157-nm (VUV) irradiation are investigated by employing a high-resolution laser calorimetric technique which allows the determination of both single- and two-photon absorptance at energy densities up to 110 mJ/cm². A strong wavelength dependence of the DUV and VUV absorption characteristics is observed: while effective two-photon absorption takes place at 193 nm, either no similar effect at all (in the case of BaF₂) or only a very minor effect (CaF₂) is observed at 157 nm. A first explanation for this absorption behaviour is given, implying the energetic band structure of CaF₂. In addition it is shown that, due to the strong nonlinear dependency, above a critical energy density the absorptance at 193 nm can exceed the absorptance at 157 nm. Furthermore, different single- and two-photon absorption coefficients are determined for different CaF₂ samples at 193 nm, indicating a two-step absorption mechanism. In addition, laser-induced aging is found in a MgF₂ sample at 193 nm, but not at 157 nm.

PACS 42.70.-a; 42.87.-d; 78.20.Ci; 42.65; 61.80

1 Introduction

The interaction of synchrotron, UV-lamp and laser radiation with dielectric crystals has been of major interest for many years. Because of their growing importance as low-absorbing UV-grade optical materials used in semiconductor microlithography, especially the alkaline and alkaline-earth fluorides have been investigated intensively [1–7].

Due to its strong correlation with the intrinsic optical properties of the crystal, the study of the electronic band structure is inevitable for a detailed understanding of the absorption mechanisms in crystals. UV spectrometric as well as photoelectron spectroscopy experiments reveal large band-gap energies of alkaline-earth fluorides, covering regions of about 9 eV (BaF₂) up to 11 eV (MgF₂) [2]. Theoretical calculations of binding energies based on the Born model [2] and the cluster model [8] were performed, as well as calculations of the electronic energy bands, using linear combination of

atomic orbitals (LCAO) [9, 10] and self-consistent field (SCF) methods [11].

At sufficiently high photon energies, nonlinear absorption processes can occur in these materials [12–14]. Two-photon absorption, for example, was observed by excitation with excimer laser radiation at 248 nm ($2h\nu = 10$ eV) and 193 nm ($2h\nu = 12.8$ eV) using high-resolution laser calorimetry [15, 16]. According to

$$A = \left| \frac{dI}{I} \right| = (\alpha_0 + \beta I) dz, \quad (1)$$

two-photon absorption results in a linear increase of absorptance A with the intensity of radiation I (α_0 and β = single- and two-photon absorption coefficients, respectively).

In addition, two-step absorption is possible via states within the forbidden zone, induced by external atoms, defects or colour centres. Including a two-step absorption mechanism, the absorptance can be written as (see the appendix and [17]):

$$A = \left(\sum_{i=1}^n \alpha_{0i} + \sum_{i=1}^n \frac{\alpha_{0i} \sigma_{2i} \eta_i \tau}{2\hbar\omega} I + \beta I \right) dz \\ = \left(\sum_{i=1}^n \alpha_{0i} + \beta_{\text{eff}} I \right) dz, \quad (2)$$

where σ_{2i} are the cross sections for absorption of the intermediate levels, η_i the efficiencies of formation of occupied intermediate levels and τ the laser-pulse length. The expression

$$\beta_{\text{eff}} = \sum_{i=1}^n \frac{\alpha_{0i} \sigma_{2i} \eta_i \tau}{2\hbar\omega} + \beta \quad (3)$$

can be regarded as an effective two-photon absorption coefficient.

In this paper, first laser calorimetric measurements of the absorptance behaviour of the alkaline-earth fluorides MgF₂, CaF₂ and BaF₂ at an irradiation wavelength of 157 nm are presented and compared with corresponding data obtained at 193 nm. Taking into account results from previous experiments at 248 nm [15] and SCF calculations of the energetic band structure of CaF₂ [11], a first simple model for the absorption mechanism can be given.

✉ Corresponding author.

Fax: +49-551/503-599, E-mail: cgoerli@llg.gwdg.de

2 Experimental setup

Absorption was determined from a quantitative laser calorimetric measurement, following the existing standard ISO 11 551 [21]. Herein, absorptance A is defined as the ratio of thermally absorbed energy Q_{abs} to total irradiation energy Q_{in} :

$$A = \frac{Q_{\text{abs}}}{Q_{\text{in}}} = \sum_i m_i c_i \frac{\Delta T}{Q_{\text{in}}}, \quad Q_{\text{in}} = \sum_{\text{burst}} Q_{\text{burst}}, \quad (4)$$

where $\sum_i m_i c_i$ represents the effective heat capacitance of sample and mount.

The experimental arrangement for the ArF excimer laser calorimeter was described in detail elsewhere [15, 22] and is similar to that of the F₂ excimer laser calorimeter, depicted schematically in Fig. 1. For the VUV wavelength of 157 nm, an F₂ excimer laser (Lambda Physik LPF 220) was used. The entire setup was installed in a vacuum chamber, which allows evacuation and subsequent N₂ purging for efficient oxygen removal. The O₂ content was kept at 0.1 ppm during the measurements, as monitored by an oxygen sensor.

The samples used for absorption measurements were CaF₂ single crystals of high purity with polished (111) surfaces grown by Korth Kristalle (Kiel, Germany) and other manufacturers, as well as BaF₂ and MgF₂ crystals of less purity. The samples had 25-mm diameter and thicknesses of 5 mm and 3 mm. They were irradiated for a time $t_{\text{irr}} = 45$ s at 157 nm and 15 s at 193 nm with repetition rates of 50, 100 and 300 Hz, respectively. The total incident energy in a burst Q_{in} was measured with a fast pyroelectric energy monitor (Laser Probe rm6600, detector RjP-637), allowing averaging over individually stored pulse energies. The irradiated areas were 4×1 mm² (157 nm) and 6×2 mm² (193 nm), respectively. By using a motor-driven variable attenuator, measurements of the absorptance at different energy densities within the range 60 mJ/cm² to 130 mJ/cm² were possible.

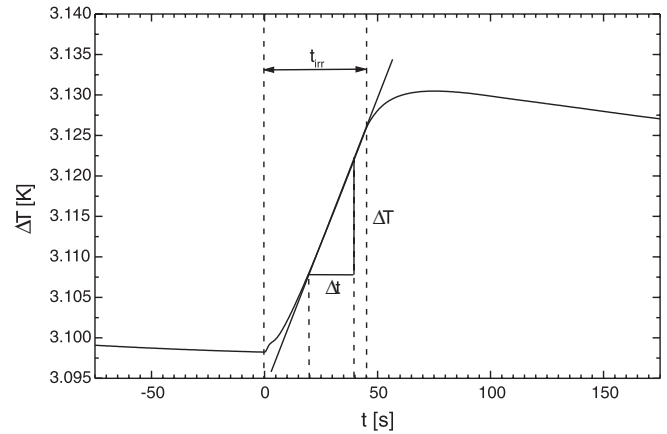


FIGURE 2 Temperature signal monitored on a CaF₂ sample during 157-nm irradiation (0–45 s). The absorptance is evaluated after drift correction in a modified gradient procedure within the time interval 20–40 s

The temperature rise ΔT was detected with an NTC sensor (Betatherm Thermistors, μK resolution) on the sample holder and determined by extrapolation from the linear part of the heating curve. Figure 2 shows as a typical example the temperature signal obtained from a CaF₂ sample irradiated at 157 nm. The corresponding linear region used for evaluation of ΔT is indicated. By electrical heating an absolute calibration of the measured absorptance could be performed [15, 21].

Previous experiments at 248 nm [23] and 193 nm showed a strong reduction of absorptance with cumulative pulse counts. This effect of laser conditioning was also observed at 157 nm. As an example, the absorption behaviour of a CaF₂ sample is drawn in Fig. 3. Initially, the absorptance has a high value of about 1.94%, which decreases nearly exponentially with the total irradiation dose until a saturation level of $A_{\text{sat}} = 1.67\%$ is reached. XPS studies and absorption measurements of LaF₃/MgF₂ systems at 248-nm and 193-nm irradiation [23–26] gave evidence that this absorption

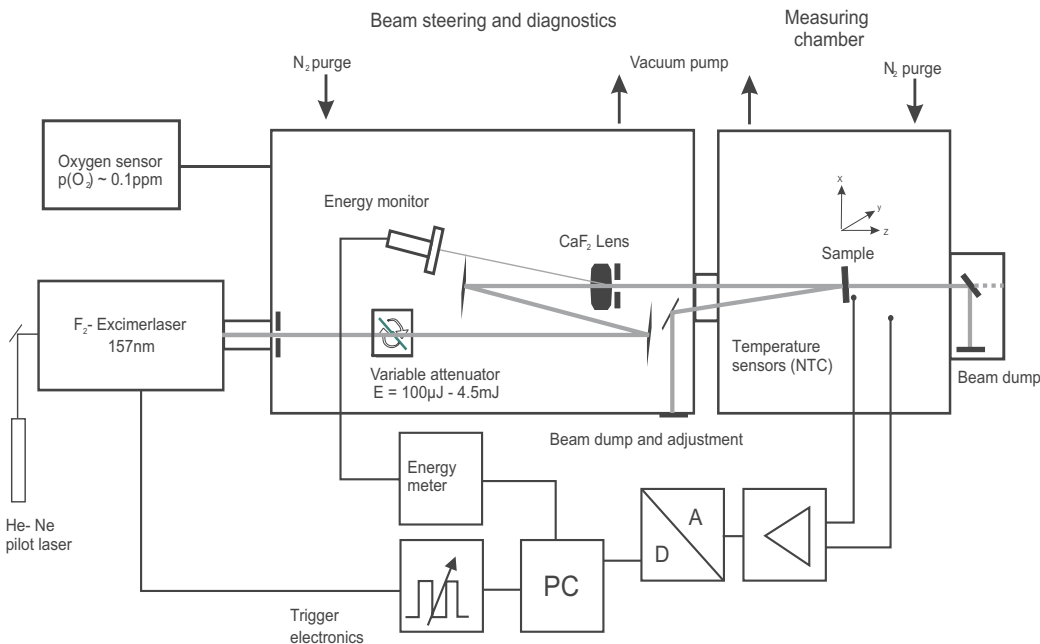


FIGURE 1 Experimental setup of the VUV absorption calorimeter. For a uniformly irradiated area on the sample, the homogeneous part of the excimer laser profile is selected by an aperture (12×4 mm²) and imaged onto the sample by a CaF₂ lens

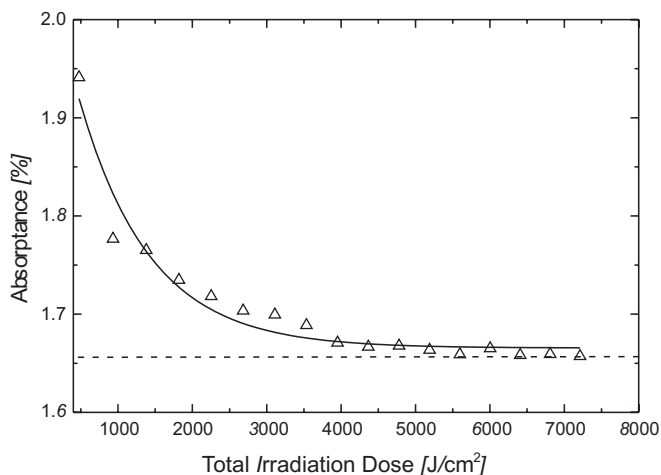


FIGURE 3 Conditioning of a CaF_2 sample at 157-nm irradiation. The absorptance decreases nearly exponentially with the total irradiation dose Q . The exponential fit $A = A_{\text{sat}} + A_0 \exp(-c/Q)$ yields a saturation level of $A_{\text{sat}} = 1.67\%$, which is approximately reached at $Q \approx 5500 \text{ J/cm}^2$

change is caused by photo-induced desorption of hydrocarbons and water from the surface (laser cleaning effect [27–30]). Thus, in order to obtain stable experimental conditions, the samples were pre-irradiated with 100 000 pulses at 157 nm ($H \approx 50\text{--}100 \text{ mJ/cm}^2$) and with 60 000 pulses at 193 nm ($H \approx 50 \text{ mJ/cm}^2$), respectively.

The DUV and VUV laser calorimeters used allow the determination of absolute absorptances with ppm (193 nm) and per-mill resolution (157 nm). As only short irradiation bursts are required, thermal loading of the samples is minimised.

3 Results and discussion

3.1 Comparison of DUV and VUV absorptance data

The absorptances of uncoated BaF_2 , CaF_2 and MgF_2 samples were measured at 193 nm and 157 nm for varying pulse energy densities. Figure 4 shows the results for two different high-purity CaF_2 samples. At both irradiation wavelengths a linear dependency of the absorptance with increasing energy density is observed. This linear behaviour of the absorptance is fully reversible, i.e. by variation of the energy density from low to high values and back the initial absorptance is reached again. However, significantly different slopes and ordinate intercepts are obtained for different wavelengths and samples.

We base the interpretation of these experimental data on (2), which has to be supplemented by the linear surface absorptance A_S :

$$A = A_S + \sum_{i=1}^n \alpha_{0i} dz + \beta_{\text{eff}} dz I = A_0 + \beta_{\text{eff}} \frac{dz}{\tau} H. \quad (5)$$

Here, A_0 describes the overall linear absorptance, which is given by the sum of surface absorptance A_S and bulk absorptance $\alpha_0 dz$ [31], β_{eff} the effective two-photon absorption coefficient and $H = \tau I$ the pulse energy density. Hence, by measuring absorptance for several energy densities H and fitting the data, it is possible to derive β_{eff} from the slope and

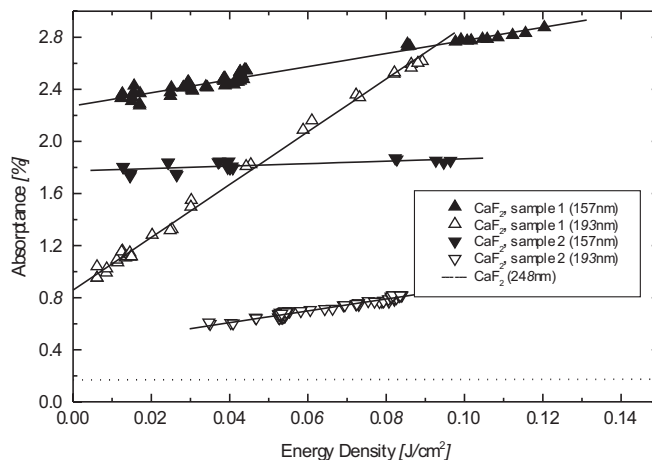


FIGURE 4 Comparison of the absorptance behaviour of two different CaF_2 samples with 5-mm thickness at 193 nm and 157 nm

A_0 from the intercept with the ordinate. A summary of coefficients obtained in this way for selected representative samples is given in Table 1.

For the CaF_2 samples shown in Fig. 4 the linear absorptance A_0 at 157 nm amounts to 2.27% (sample 1) and 1.77% (sample 2). These values are three to four times higher in comparison with the results at 193 nm (0.86% for sample 1 and 0.43% for sample 2, respectively), since the excitation takes place closer to the conduction states and the probability for the absorption process is increased at 157 nm.

Regarding the band gap of CaF_2 ($E_G = 10 \text{ eV}$), two-photon absorption should be possible at 193 nm ($2h\nu = 12.8 \text{ eV}$) and, indeed, a linear increase of absorptance with energy density is evident. This increase is transient, as low-intensity absorption is identical before and after high-intensity irradiation. The different values obtained for the effective two-photon absorption coefficients β_{eff} ($5.7 \times 10^{-9} \text{ cm/W}$ for sample 1 and $1.3 \times 10^{-9} \text{ cm/W}$ for sample 2) support the model of a two-step mechanism as discussed in detail later (cf. Sect. 3.2).

In contrast to the measurements at 193 nm, the absorptance at 157 nm obviously depends only very weakly on the applied energy density. The low β_{eff} values of about $1.4 \times 10^{-9} \text{ cm/W}$ (sample 1) and $0.3 \times 10^{-9} \text{ cm/W}$ (sample 2) reflect this fact, indicating a rather weak nonlinear two-photon absorption behaviour. For comparison, Fig. 4 also

Material	E_G [eV]	$A_0^{(193 \text{ nm})}$ [%]	$A_0^{(157 \text{ nm})}$ [%]	$\beta_{\text{eff}}^{(193 \text{ nm})}$ [10^{-9} cm/W]	$\beta_{\text{eff}}^{(157 \text{ nm})}$ [10^{-9} cm/W]
CaF_2	10				
sample 1		0.86	2.27	5.7	1.4
sample 2		0.43	1.77	1.3	0.3
sample 3		1.36	–	8.4	–
sample 4		1.45	–	8.2	–
BaF_2	9	1.23	8.49	1.2	0
MgF_2	11	–	5.19	–	1.0

TABLE 1 Effective linear and nonlinear absorptance coefficients of alkaline-earth fluorides at 193 nm and 157 nm (thickness: 5 mm). Due to degradation of MgF_2 at 193-nm irradiation, no values could be determined in this case

shows the absorbance of a CaF₂ sample measured earlier at the wavelength of 248 nm [15]. In this case, a constant absorbance was observed on a rather low level (about 0.17%) over a wide range of energy densities (up to 2 J/cm²).

Furthermore, Fig. 4 suggests that the strong nonlinear absorbance behaviour of CaF₂ at 193 nm and the nearly constant absorbance at 157 nm lead to a crossing point between these two curves, so that beyond a critical energy density the absorbance at 157 nm could be lower than at 193 nm. The position of the crossing point depends obviously on the specific sample; while for sample 1 the critical energy density amounts to about 0.09 J/cm², for sample 2 the value is significantly higher (> 0.3 J/cm²).

In Fig. 5 the absorbance behaviour of BaF₂ and MgF₂ is shown. The linear absorbance A₀ for BaF₂ at 157 nm (8.49%) is seven times higher than the value at 193 nm (1.23%) and four to five times higher than for CaF₂ (cf. Table 1). This

is attributed to the smaller band gap (9 eV) and to possible impurities. Similar statements as in the case of CaF₂ can be made concerning the absorption mechanism: no two-photon absorption is observable at 157 nm ($\beta_{\text{eff}} \approx 0$), whereas β_{eff} at 193 nm amounts to 1.2×10^{-9} cm/W. At 157 nm MgF₂ shows a higher linear absorbance (A₀ = 4.96%) than CaF₂. This indicates the large influence of crystal defects and impurities, since the gap of 11 eV is larger than in the case of CaF₂ (10 eV). The coefficient β_{eff} is also relatively weak ($\approx 1 \times 10^{-9}$ cm/W).

From all these measurements it can be concluded that two-photon absorption in CaF₂ and BaF₂ is obviously only a relevant process for 193-nm radiation. A first explanation of this effect based on the energetic band structure of CaF₂ will be given in the following.

Figure 6 shows the calculated electronic band scheme of CaF₂, replotted from Heaton and Lin [11]. The valence

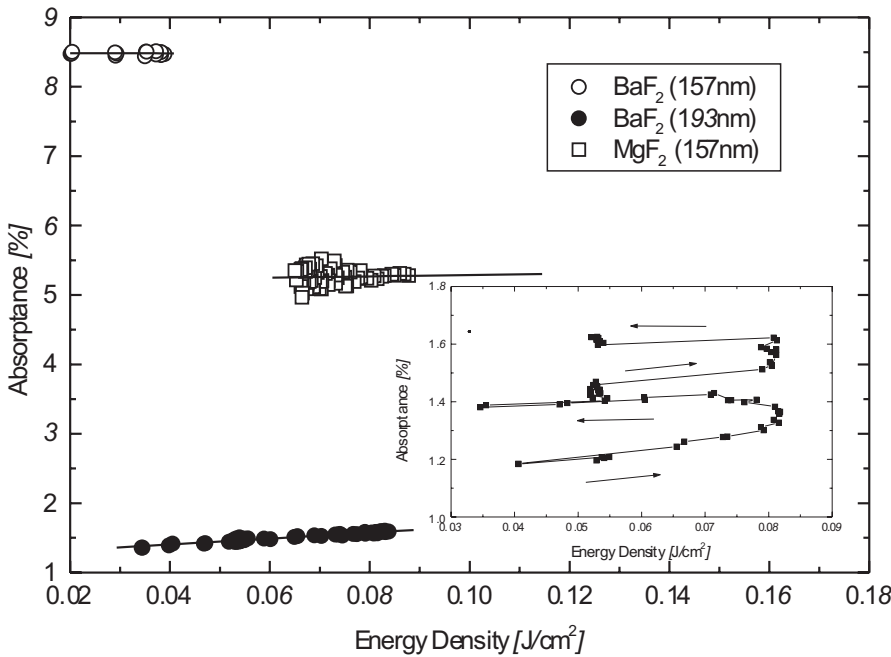


FIGURE 5 Absorbance behaviour of a BaF₂ and a MgF₂ sample (5 mm), measured at 193 nm and 157 nm. The inset shows the degradation of MgF₂ at 193-nm irradiation. The arrows assign the chronological order of irradiation

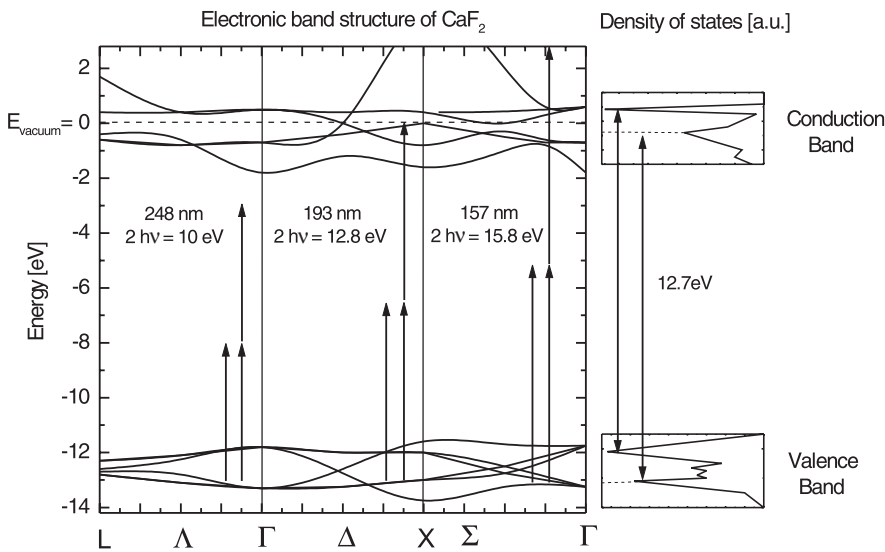


FIGURE 6 Electronic band structure and densities of states in CaF₂ (redrawn from [11]). The arrows denote the photon energy for single- and two-photon absorption. Different positions of the arrows are for clarity only

band (VB) is located about -12.5 eV below the vacuum energy level with a width of nearly 1.5 eV. Its structure is strongly dominated by the $F^-(2p)$ orbitals. The density of states (DOS) has a local maximum at -13.1 eV and a global maximum at -12.1 eV in the VB, which is in good agreement with the onset of photo-emission of about 10.5 eV [2]. The conduction band (CB), in the lowest parts originating mainly from the $Ca(4s)$ orbitals, is close to the vacuum level with DOS maxima at -0.41 eV and 0.4 eV. At Γ the direct band gap energy amounts to 10 eV; the absolute minimum (9.8 eV) is located at X.

Due to the double photon energy of about 10 eV at 248 nm, two-photon absorption processes promoting an electron from the VB into the CB should not be possible or at least weakly occur. This is in agreement with previous experiments [15]. In contrast, at 193 nm transitions between -13.1 eV and -0.4 eV are most probable (cf. DOS distributions shown in the right-hand part of Fig. 6), yielding a resonant energy of 12.7 eV. This theoretically supports the possibility of an effective two-photon excitation at 193 nm and explains the observed experimental data.

In the case of 157-nm radiation, however, the combined energy of two photons (15.8 eV) exceeds the vacuum level. Thus, depending on the valence-band state, the electron receives a kinetic energy of about 3 to 4 eV. Near the surface, the electron is able to leave the crystal lattice and can be detected as a photoelectron [5]. In the bulk, energy trapping by self-trapped-exciton (STE) formation occurs [18]. The STE can then decay in a radiative way by broadband recombination fluorescence, whereby the remaining elastic deformation is removed by excitation of phonons. Other decay channels are nonradiative recombination into the undisturbed lattice and formation of stable F and H centres [18].

Since phonons contribute to thermal heating of the crystal and therefore to the calorimetrically determined absorption, it is concluded from the lack of two-photon absorption at 157-nm excitation that thermal relaxation is suppressed in comparison with fluorescence emission. This is in agreement with conclusions for recombination of core excitons drawn from far-ultraviolet reflectance spectra [1] and our first spectroscopic studies of STE fluorescence in alkaline-earth fluorides at 193 nm and 157 nm [32]. However, to confirm this assumption, further investigations of the wavelength dependence of the absorption behaviour in fluoride crystals as well as precise transmission and spectroscopic measurements are necessary.

3.2 Correlation between single- and two-photon absorption in CaF_2

In order to clarify the nature of the two-photon absorption mechanism at 193 nm, the intensity-dependent absorptance of 19 CaF_2 samples from different vendors with 5-mm and 3-mm thickness was determined. The evaluated coefficients A_0 and β_{eff} are plotted versus each other in Fig. 7. For comparability of the data obtained from 3-mm samples with those from 5-mm samples it was considered, in a first approximation, that the surface absorptance is negligibly small in comparison with the bulk absorptance; thus, an extrapolation

from 3-mm to 5-mm data was performed by multiplying the coefficients A_0 and β_{eff} with a factor 5/3.

As was pointed out in the introduction (cf. (3)), a correlation between α_0 and β_{eff} can be regarded as a strong indication for a two-step mechanism. Indeed, in Fig. 7 an approximate proportionality between A_0 and β_{eff} can be seen. Note that according to (3) this linear relationship is only expected if σ_{2i} and η_i are assumed to be constant, i.e. impurities and defects inside the crystal are of the same kind and quantity. It is important to mention that high (low) values for α_0 do not automatically yield a corresponding high (low) value for β_{eff} , since σ_{2i} and η_i may vary depending on the specific nature of the impurities or defects. On the other hand, a low value of α_0 is a necessary (but not a sufficient) condition for low β_{eff} .

The intercept of the fit line with the ordinate represents the case of intrinsic two-photon absorption, since this corresponds to the limit $\alpha_0 \rightarrow 0$ and thus $\beta_{\text{eff}} \rightarrow \beta$. This procedure yields a rough upper boundary for the intrinsic two-photon absorption coefficient β of about 1.5×10^{-9} cm/W. However, as can be seen in Fig. 7, there are also samples with smaller values ($\beta_{\text{eff}} \approx 1 \times 10^{-9}$ cm/W).

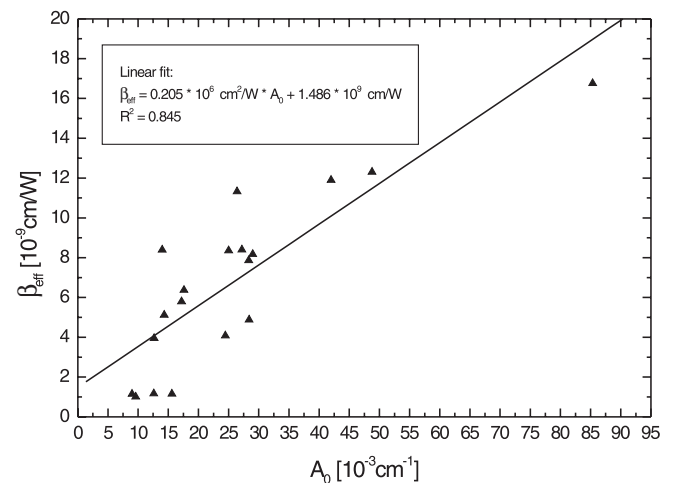


FIGURE 7 Correlation between nonlinear and linear absorptance coefficients for different CaF_2 samples. The linear fit corresponds to (3) for constant σ_{2i} and η_i

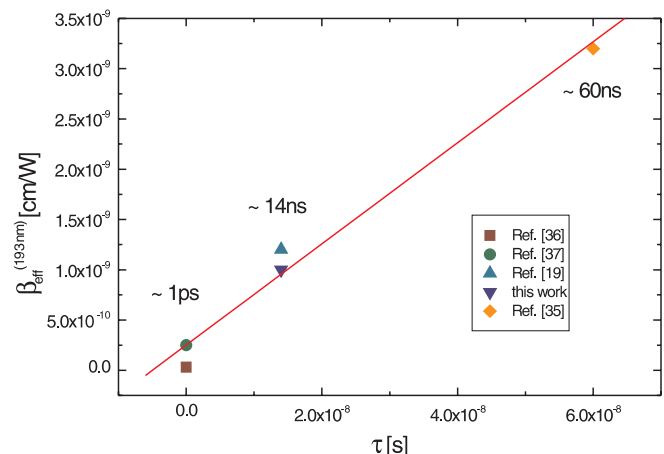


FIGURE 8 Comparison of two-photon absorption coefficients obtained for CaF_2 at 193 nm for different laser-pulse lengths τ

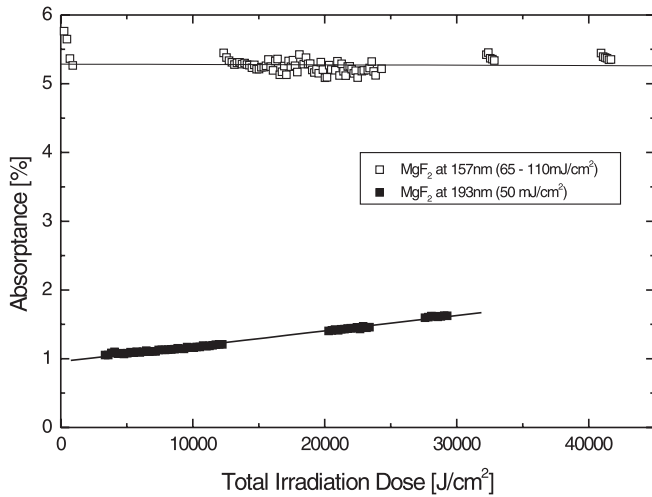


FIGURE 9 Absorbance versus cumulative irradiation dose of a 5-nm MgF₂ sample irradiated with energy densities of about 65–110 mJ/cm² (157 nm) and 50 mJ/cm² (193 nm), respectively. The sample shows irreversible degradation at 193 nm, whereas no aging is observed at 157 nm

Comparing these values of the purest samples with literature data determined for *ps* and *ns* pulses at 193 nm [19, 33–35], a linear correlation between β_{eff} and the pulse length τ is evident (Fig. 8), as expected from (3). This result confirms the two-step mechanism as the most important two-photon process for *ns* and *ps* excitation in CaF₂.

3.3 Degradation

In addition to linear and second-order nonlinear absorbance, samples can also undergo cumulative changes upon laser irradiation, e.g. degradation due to colour-centre formation. In this case the linear relationship according to (5) does not hold any longer. As an example of such a laser-induced degradation effect the absorbance behaviour of a MgF₂ sample during energy-density variation is shown in the inset of Fig. 5. In addition, Fig. 9 displays absorbance measurements of the same sample versus the total irradiation dose. Irradiation at 193 nm (energy density \approx 50 mJ/cm²) leads to a linear increase of absorbance. In contrast to the absorbance behaviour of CaF₂ and BaF₂, this is an irreversible process. Therefore, a determination of absorption coefficients at 193 nm was not possible. Probably degradation is due to the formation of strongly absorbing colour centres, as observed in MgF₂ at 248 nm for single-photon absorption [36]. The nature of the colour centres, e.g. F, M or V_K centres, is a subject of future spectroscopic investigations.

Surprisingly, no aging could be observed during 157-nm irradiation (cf. upper curve in Fig. 9). Regarding the band-gap and photon energies, this might be an indication that laser-induced colour-centre formation is caused by two-photon absorption with absorbing states near the lowest conduction states.

4 Conclusion

Concerning the results of calorimetric absorbance measurements of alkaline-earth fluorides at 193 nm and 157 nm, it can be concluded that single-photon absorption at

157 nm is a few times higher than at 193 nm, which is attributed to the excitation closer to the band edge. Two-photon absorption is observed mainly at 193-nm irradiation, where an effective excitation of electrons from the valence band into the conduction band is possible. At 157 nm, only a weak non-linear absorption behaviour is observed. This is in agreement with calculated band structures of alkaline-earth fluorides. In addition, this leads to the effect that, above a critical energy density, absorbance at 193 nm is higher than at 157 nm.

It can be shown that there is a strong indication for two-photon absorption as a two-step process. This was deduced from the rough proportionality $\beta_{\text{eff}} \propto A_0$ for different CaF₂ samples and the linear relationship between β_{eff} and τ . Irreversible aging of MgF₂, which occurs only at 193 nm, was attributed to the formation of colour centres via a two-photon absorption process. However, in order to support these assumptions, spectroscopic analysis of laser-induced fluorescence and supplementing transmission measurements are necessary. Corresponding work is in progress.

Appendix

In the case of linear two-step absorption, Lambert–Beer’s law reads

$$\frac{dI}{dz} = -(\sigma_1 N_1 + \sigma_2 N_2)I = -(\alpha_0 + \sigma_2 N_2)I, \quad (\text{A.1})$$

where N_i is the number of absorbing species per volume unit that can be promoted into the level i and σ_i the respective cross section. The rate of formation of electrons in level 1, which can be raised into level 2 by absorption of a second photon, is

$$\frac{dN_2}{dt} = \frac{\alpha_0 \eta I}{\hbar \omega}, \quad (\text{A.2})$$

with the single-step absorption efficiency η . This yields

$$\frac{dI}{dz} = -\left(\alpha_0 + \frac{\alpha_0 \sigma_2 \eta t}{\hbar \omega} I\right) I. \quad (\text{A.3})$$

Integration from $t = 0$ to τ (rectangular pulse shape assumed) and summation over n intermediate levels leads to the two-step part of the absorbance in (2).

ACKNOWLEDGEMENTS This work was supported by the Bundesministerium für Bildung und Forschung under Grant No. 13EU0158 as part of the EUREKA project CHOCLAB II (EU 2359). The authors wish to thank I. Dreger from Max-Planck-Institut für biophysikalische Chemie, Göttingen for critically reading the manuscript.

REFERENCES

- 1 G.W. Rubloff: Phys. Rev. B **5**, 662 (1972)
- 2 R.T. Poole, J. Szajman, R.C.G. Leckey, J.C. Jenkins, J. Liesegang: Phys. Rev. B **12**, 5872 (1975)
- 3 A. Ejiri, S. Kubota, K. Yahagi: J. Phys. Soc. Jpn. **64**, 1484 (1995)
- 4 M.A. Terekhin, I.A. Kamenskikh, V.N. Makhov, V.A. Kozlov, I.H. Munro, D.A. Shaw, C.M. Gregory, M.A. Hayes: J. Phys.: Condens. Matter **8**, 497 (1996)
- 5 M. Huisinga, M. Reichling, E. Matthias: Phys. Rev. B **55**, 7600 (1997)
- 6 E. Stenzel, S. Gogoll, J. Sils, M. Huisinga, H. Johansen, G. Kastner, M. Reichling, E. Matthias: Appl. Surf. Sci. **109–110**, 162 (1997)

- 7 I. Becker, J.Y. Gesland, N.Yu. Kirikova, V.N. Makhov, M. Runne, M. Queffelec, T.V. Uvarova, G. Zimmerer: *J. Luminesc.* **78**, 91 (1998)
- 8 T. Ikeda, H. Kobayashi, Y. Ohmura, H. Nakamatsu, T. Mukoyama: *J. Phys. Soc. Jpn.* **66**, 1074 and 1079 (1997)
- 9 R. Evarestov, I.V. Murin, A.V. Petrov: *J. Phys: Condens. Matter* **1**, 6603 (1989)
- 10 J.P. Albert, C. Jouanin, C. Gout: *Phys. Rev. B* **16**, 4619 (1977)
- 11 R.A. Heaton, C.C. Lin: *Phys. Rev. B* **22**, 3629 (1980)
- 12 W. Kaiser, C.G. Garrett: *Phys. Rev. Lett.* **7**, 229 (1961)
- 13 P. Liu, R. Yen, N. Bloembergen: *Appl. Opt.* **18**, 1015 (1979)
- 14 P. Liu, W.L. Smith, H. Lotem, J.H. Bechtel, N. Bloembergen: *Phys. Rev. B* **17**, 4620 (1978)
- 15 E. Eva, K. Mann: *Appl. Phys. A* **62**, 143 (1996)
- 16 O. Apel: *Dissertation, Universität Göttingen* (Cuvillier, Göttingen, Germany 2000)
- 17 D.P. Dvornikov, E.L. Ivchenko, V.V. Pershin, I.D. Yaroshetskij: *Sov. Phys. Semicond.* **10**, 1374 (1976)
- 18 K.S. Song, R.T. Williams: *Self-trapped Excitons* (Springer Ser. Solid State Sci. **105**) (Springer, Berlin 1993) and references therein
- 19 E. Eva: *Dissertation, Universität Göttingen* (Cuvillier, Göttingen, Germany 2001)
- 20 E. Eva, K. Mann: *Proc. SPIE* **2966**, 72 (1997)
- 21 ISO/DIS 11 551: 'Test method for absorbance of optical laser components'
- 22 O. Apel, K. Mann, A. Zöller, R. Goetzelmann, E. Eva: *Appl. Opt.* **39**, 3165 (2000)
- 23 E. Eva, K. Mann: *Appl. Opt.* **35**, 5613 (1996)
- 24 B. Li, S. Martin, E. Welsch: *Opt. Lett.* **24**, 1398 (1999)
- 25 B. Li, S. Martin, E. Welsch: *Appl. Opt.* **39**, 4690 (2000)
- 26 J. Heber, R. Thielsch, H. Blaschke, N. Kaiser, U. Leinhos, R. Görtler: *Proc. SPIE* **3578**, 83 (1999)
- 27 D.J. Krajnovich, M. Kulkarni, W. Leung, A.C. Tam, A. Spool, B. Yorck: *Appl. Opt.* **31**, 6062 (1992)
- 28 A. Bodemann, N. Kaiser: *Proc. SPIE* **2714**, 405 (1996)
- 29 N.S. McIntyre, R.D. Davidson, T.L. Walzak, R. Williston, M. Westcott, A. Pekarsky: *J. Vac. Sci. Technol. A* **9**, 1355 (1991)
- 30 K. Yamaguchi, Y. Uematsu, Y. Ikoma, F. Watanabe, T. Motooka, T. Igarashi: *J. Vac. Sci. Technol. B* **15**, 277 (1997)
- 31 E. Eva, K. Mann: *Appl. Surf. Sci.* **109**, 52 (1997)
- 32 C. Görling, U. Leinhos, K. Mann: to be published
- 33 E. Eliseev, E. Fadeeva: *J. Opt. Technol.* **63**, 136 (1996)
- 34 K. Mossavi, T. Hofmann, G. Szabo, F. Tittel: *Opt. Lett.* **18**, 435 (1993)
- 35 O. Kittelmann, J. Ringling: *Opt. Lett.* **19**, 2053 (1994)
- 36 A.J. Taylor, R.B. Gibson, J.P. Roberts: *Opt. Lett.* **13**, 814 (1988)